OBSERVATIONS OF ROCK FABRIC CONTROLS ON THE ELECTRICAL PROPERTIES OF SANDSTONES

by Gerald A. LaTorraca
Connie G. Hall

ABSTRACT

We report electrical properties measurements on 323 sandstone samples with minimal amounts of predominantly authigenic clays. All measurements were made at Chevron during the past 15 years using net effective reservoir pressure and room temperature. Almost all of the samples are fairly well consolidated. The most common clay is kaolinite with lesser amounts of illite, chlorite, glauconite, and traces of smectite. Our objectives in this paper are to document the ranges of the cementation (**m**) and saturation (**n**) exponents in our data and to relate the values of **m** and **n** to rock fabric.

We "clay corrected" the measured values of resistivity index (**RI**) and formation factor (**F**) using the Waxman-Smits equations (1968) and the B value from Juhasz (1981) to obtain $\mathbf{F^*}$, $\mathbf{RI^*}$, $\mathbf{m^*}$ and $\mathbf{n^*}$, the clay corrected cementation and saturation exponents. These clay corrections are typically less than 0.05 to **m** and 0.1 to **n**. Henceforth, we shall refer only to the "clay corrected" or geometric parameters: $\mathbf{F^*}$, $\mathbf{RI^*}$, $\mathbf{m^*}$ and $\mathbf{n^*}$.

For the distribution of $\mathbf{m^*}$, 95% of the values are between 1.7 and 2.1 with a sharp peak between 1.8-1.9. Consistent with prior observations (e.g. Wyllie and Gregory, 1953), the relatively small variation in $\mathbf{m^*}$ appears to be controlled by grain shape and cementation.

The values of $\mathbf{n^*}$ are broadly distributed between 0.6 and 2.6. The large variation in $\mathbf{n^*}$ appears to be related to cementation, pressure solution, and depositional environment (e.g. laminations).

Samples without visible laminations, as identified from thin-section photographs, have $\mathbf{n^*}$ values ranging from 1.0 to 2.6. Such samples with low values of $\mathbf{n^*}$ tend to have an appreciable fraction of their pore volumes consisting of well-connected, hairline pores. Because of their high capillarity, these pores remain brine saturated high in the hydrocarbon column and act to preserve conductivity as brine is drained from the rock.

Finely-laminated, aeolian sandstones tend to have low saturation exponents, i.e., $0.6 \leq \mathbf{n^*} \leq 1.4$. Their $\mathbf{n^*}$ values are strongly correlated to the inverse of the minimum brine saturation attained during desaturation. Such low values of $\mathbf{n^*}$ are consistent with a simple model which accounts for systematic variations in capillary pressure and brine saturation in laminated samples.

The value of $\mathbf{n^*}$ in our dataset is fairly well correlated with porosity. This correlation is useful for establishing bounds on $\mathbf{n^*}$.

CEMENTATION EXPONENTS IN CLEAN SANDSTONES

The Formation Factor (F^*) of a sample is a measure of how efficiently the pore space is distributed for electrical conduction. In the extreme of zero efficiency, if the porosity(Ø) were concentrated in a blob inside the sample with no connections to the surfaces of the sample, there would be no conduction and F^* would be infinite. Alternatively, the most efficient distribution of porosity occurs when all the pore space is concentrated in a through going tube or fracture. There the Formation Factor (F^*) would be at a minimum for that porosity and the cementation exponent m^* would be at its minimum value of 1. Any changes in cross-section of the tube or fracture would result in reduced conduction and increased F^* and m^*, assuming that the porosity remained unchanged. The porosity in most sandstones is intergranular, i.e., between the grains, and the electrical conduction paths much less uniform than through a tube. The simplest model of intergranular porosity is a bead pack. For periodic, cubic arrays of beads, Shen et al.(1990) showed that the value of m^* lies between 1.3 and 1.5. These simple structures probably have the lowest m^* values we can expect for grain supported sandstones. Most sandstones have more complicated fabrics than that of beadpacks with the consequences of higher F^* values for the same porosity and values of $m^*>1.5$. Archie (1942) found the cementation exponent to vary between 1.8 and 2.0 for consolidated sandsones. Our laboratory data are consistent with this observation.

Distribution of m* Values

The distribution of m^* values measured at Chevron is shown in histogram form as Figure 1. Almost all of the m^* values fall within the range of $m^* = 1.7$ to 2.1 and the distribution of values is sharply peaked between 1.8 and 1.9. The average value of m^* is 1.87 with a standard deviation of 0.10. The narrow range of m^* values appears to reflect a narrow range of pore geometries (as opposed to pore sizes) for these fairly "clean" sandstones.

Of the 323 samples, 164 came from Reservoir A, a Jurassic, deltaic sandstone. Samples from Reservoir A have an average m^* value of 1.89 with a standard deviation of 0.09 (Figure 2).Without samples from Reservoir A, the average value of m^* is 1.85 with a standard deviation of 0.10 (Figure 3). Thus, the average value of m^* for the complete dataset is slightly biased upward by the data from Reservoir A. Figure 4 is a crossplot of F^* versus Ø for the complete dataset.

Fabric Controls on a* and m*

When the power law relationship between Formation Factor and porosity is calculated for an individual sample, only the value of m^* can be determined (one equation, one unknown). When the power law relationship between Formation Factor and porosity is evaluated for a suite of samples, the values of both a^* and m^* are determined by regression methods. The use of two parameters (a^* and m^*) yields a better fit to the data than can be obtained with a single parameter (m^*). Typically, a^* and m^* values are determined on a suite of samples from the same formation or lithofacies. When the pore geometry is changing with porosity, the values of a^* and m^* can take on odd values as they do for the Fontainebleau sandstone. Figure 5 is a crossplot of F versus Ø for four Fontainebleau samples. Porosity ranges from 5-22% and the value of a^* is calculated to be 0.13 and m^* is 2.8.

We propose that these apparently odd values of $\mathbf{a}^*$ and $\mathbf{m}^*$ in Fontainebleau sandstones reflect increased cementation and randomly scattered large pores in the low porosity samples. Examination of the Fontainebleau samples in thin-section reveals that the higher porosity samples have minimal quartz overgrowths while the lower porosity samples have extensive quartz overgrowths (Figure 6). The $\mathbf{m}^*$ values calculated for three of the samples are shown to the right of the corresponding photomicrographs. Because cementation appears to have occurred non-uniformly, the pore sizes and pore connections in the low porosity samples are more variable in cross-section than in the high porosity samples. Note the increase in $\mathbf{m}^*$ with increasing cementation.

The increase in $\mathbf{m}^*$ due to cementation can be predicted by the grain consolidation model of Roberts and Schwartz (1985) and Schwartz and Kimminau (1987). They allow the grains to grow in the pore space of a dense random packing of spherical grains. They add a randomness to this grain growth such that not every grain undergoes cementation uniformly. The result is that grain growth reduces the porosity and changes the shape of most pores but allows some pores to remain large. This growth process results in an increase in $\mathbf{m}^*$ as porosity is decreased, due partly to the changes in pore shape and partly to the generation of "isolated" patches of porosity. The isolated patches, which occur in cemented rocks, contribute relatively little to conduction but can be a major part of the porosity.

Observing that cementation resulted in a low value of $\mathbf{a}^*$ and a high value of $\mathbf{m}^*$ for the Fontainebleau sandstone, we suggest that values of $\mathbf{a}^*<1$ are to be expected for groups of samples in which cementation is increasing with decreasing porosity. This effect may also be seen in Figure 4. There, we applied a reduced major axis (RMA) regression to all of our formation factor and porosity measurements and calculated values of $\mathbf{a}^*=0.84$ and $\mathbf{m}^*=1.97$.

SATURATION EXPONENTS IN SANDSTONES

Distribution of n* Values

The samples in this study are from 11 different oil fields and 1 quarry. Figure 7 is a histogram of $\mathbf{n}^*$ values for all of the 295 samples. The $\mathbf{n}^*$ values vary between 0.6-2.6 and exhibit a strong peak in the 2.0-2.2 range. The 295 samples include 145 Jurassic, deltaic sandstones from Reservoir A and 47 Triassic, aeolian sandstones from Reservoir B. Because these samples had a strong influence on the distribution of $\mathbf{n}^*$ values, we separated the samples into the three groups: Reservoir A sandstones, Reservoir B sandstones and sandstones from the other reservoirs.

For Reservoir A samples, the $\mathbf{n}^*$ values fall in the range of 1.4-2.6 (Figure 8) with most values between 2.0 and 2.2. For the aeolian sandstones from Reservoir B, which tend to be thinly laminated, the $\mathbf{n}^*$ values range from 0.6-1.4 (Figure 9).

When the data from Reservoirs A and B are removed (Figure 10), the distribution of $\mathbf{n}^*$ values is more uniform i.e., the strong peaks at 1.1-1.2 and 2.0-2.2 are gone. This group of samples has $\mathbf{n}^*$ values between 1.0-2.5, with the majority of $\mathbf{n}^*$ values in the range of 1.4-2.0. We infer from this data that even though a given field may have characteristic $\mathbf{n}^*$ values, these values are difficult to predict without core measurements or knowledge of the rock fabric.

Rock Fabric Effects on n*

We do not see a strong correlation between sorting and the value of **n***, based on visual estimates of sorting from thin-sections. Well-sorted samples appear just as likely to have low (or high) **n*** values as do poorly-sorted samples.

To date, 196 samples have been separated into two categories (i.e., sandstones without visible laminations and laminated sandstones) based on rock fabric from thin-section and hand specimen observations. Of the 196 samples, 75 have been identified as homogeneous. For the homogeneous samples, the **n*** values are between 1.0-2.6, with an average value of 1.92. When the homogeneous samples from Reservoir A are removed, the **n*** range does not change much (1.0-2.5), although the average value of **n*** is reduced to 1.80.

Homogeneous samples with **n*** values in the 1.0 to 1.6 range tend to be fine-grained and low porosity (<15%). Thin-section photomicrographs for two samples from this group are shown in Figure 11. These samples have a large number of hairline pores along grain contacts (apparently caused by pressure solution). We speculate that during desaturation, these pores will tend to remain brine saturated and leave a well-connected conduction path nearly as efficient as when the pores were filled with brine. However, some fine-grained, homogeneous samples with higher porosities have high **n*** values (Figure 12). Consequently, we cannot infer that a sample has a low **n*** just because it is fine-grained. Unlike the previous samples with low **n*** values, a minor fraction of the pore volume consists of well-connected, hairline pores along grain contacts. Thus, brine connections between pores will be more easily broken during desaturation with the result of higher values of **n***.

Model For the Saturation Exponent of Laminated Sandstones

The low values of $\mathbf{n}^*$ for finely laminated core are caused by variations in brine saturation from lamina to lamina within the samples. To illustrate this point, consider what happens at the same height above the oil-water contact in a sandstone with interspersed fine and coarse grained laminae, all with about the same porosity. The capillary pressure curves for the two lamina types would exhibit quite different saturations for a given capillary pressure. The fine-grained laminae will tend to have a higher brine saturation and thus be more conductive than the coarser grained laminae. The bulk resistivity of the laminated sample is the parallel (or harmonic) mean of the resistivities of the laminae weighted by their volumes, while the brine saturation is the arithmetic average of the brine saturations of the laminae (also weighted by their volumes).

For a numerical example of the lowering of $\mathbf{n}^*$ due to laminations, suppose half of a sample consists of coarse-grained laminae and half of the sample fine-grained laminae, and the formation factors and porosities of all the laminae are the same. At some height above the oil-water contact, the coarse-grained half would have a saturation of 20% and the fine-grained half a saturation of 80% (Figure 13). The average brine saturation is 50%. If both halves had a saturation exponent of $\mathbf{n}^*$=1.8, then the $\mathbf{RI}^*$s of the fine- and coarse-grained halves would be 1.49 and 18.12, respectively. The composite $\mathbf{RI}^*$, obtained by averaging the reciprocals of the $\mathbf{RI}^*$s for each half, is 2.76. The saturation exponent is obtained by using the average brine saturation of the two halves and the composite $\mathbf{RI}^*$, with the result that $\mathbf{n}^*$=1.47 for the composite. Thus, the resistivity and the saturation exponent for the composite are lower than the resistivity and saturation exponent would be for either of the

two halves at a saturation of 50%. Based on this simple analysis, then, the value of $\mathbf{n^*}$ will tend to be lower for laminated sandstones than for homogeneous sandstones.

Curvilinear RI*-Sw Crossplots for Laminated Samples

If we follow the same logic to calculate $\mathbf{RI^*}$ and $\mathbf{S_w}$ at a series of points for a laminated sample, we find that the $\mathbf{RI^*}$-$\mathbf{S_w}$ curve can no longer be represented by a simple power law relationship i.e. the $\mathbf{RI^*}$-$\mathbf{S_w}$ crossplot is no longer linear on a log-log plot, but can exhibit significant curvature.

Figure 14 is a plot of $\mathbf{RI^*}$ versus $\mathbf{S_w}$ for two laminated samples. These data exhibit the most curvature we have seen in $\mathbf{RI^*}$-$\mathbf{S_w}$ plots. Note that at high brine saturations, the slope of the crossplotted data is low (low $\mathbf{n^*}$ value), while at lower brine saturations the slope is steeper (larger $\mathbf{n^*}$). Thus, if similar samples are desaturated to only 60-70%, they will appear to have low $\mathbf{n^*}$ values. This condition of high minimum brine saturation occurs for low permeability, laminated samples from Reservoir B. These samples require higher capillary pressures to drive them to low brine saturations than are provided by the thickness of the hydrocarbon column. Such samples are, consequently, desaturated only to fairly high brine saturations and exhibit low values of $\mathbf{n^*}$. In Figure 15, we crossplotted the clay-corrected saturation exponent $\mathbf{n^*}$ versus the minimum brine saturations attained in the finely-laminated samples from Reservoir B. Note the trend toward higher values of $\mathbf{n^*}$ for low, minimum brine saturations. This trend is consistent with the curvature in the $\mathbf{RI^*}$-$\mathbf{S_w}$ plot of Figure 14.

Photo-micrographs of Laminated Samples with Low Saturation Exponents

Figures 16-17 are photomicrographs of thin-sections of laminated, aeolian sandstones from Reservoir B. The figures are annotated with the values of $\mathbf{n^*}$ measured on each sample. The sample with the higher $\mathbf{n^*}$ value (Figure 16) has essentially two grain sizes, i. e. laminae of either fine grains or medium grains. This geometry has resulted in a moderate contrast in capillarity between the laminae. Consequently, both types of lamina could be desaturated to fairly low brine saturations and there was only a moderate lowering of the value of $\mathbf{n^*}$ calculated from the $\mathbf{RI^*}$-$\mathbf{S_w}$ crossplot.

The sample with the lower $\mathbf{n^*}$ value (Figure 17) has a lower average grain size and broader distribution of grain sizes in the laminae. The laminae tend to be either medium-grained and well-sorted or poorly sorted with grain sizes ranging from extremely fine-grained to medium-grained. This sample has a large contrast in capillarity between the laminae such that the poorly sorted laminae probably remained fully brine saturated at even the highest capillary pressures used to desaturate the sample. Consequently, the minimum brine saturation attained during desaturation was high and the value of $\mathbf{n^*}$ low.

Correlations of n*_with Porosity

Figure 18 shows that there is a fair trend between $\mathbf{n^*}$ and $\mathbf{\emptyset}$ in the Chevron dataset. Although the correlation is not strong enough to build a reliable estimate of $\mathbf{n^*}$ from porosity, there are useful bounds which we can put on $\mathbf{n^*}$ for a given porosity. The apparent trend between $\mathbf{n^*}$ and $\mathbf{\emptyset}$ has significant economic implications. In higher porosity formations, the calculated brine saturation will not vary much whether $\mathbf{n^*}$ is 2 or 2.5. However, in low porosity formations, where a low initial brine saturation is usually required for the field to be economic, knowing whether $\mathbf{n^*}$ is 1 or 2 can be critical to the

economic evaluation of the field. For example, if RI^*=5, then S_w=20% for n^*=1 and S_w=45% for n^*=2.

DISCUSSION

Summary

The electrical properties data presented represent more than 15 years of measurements made in the same laboratory at Chevron. The cementation exponent m^* is seen to vary over a narrow range of values while the saturation exponent n^* varies over a wide range. We inferred that pore shape is the major factor controlling m^* and that pore shape, pore size and heterogeneities such as laminations can all exert significant controls on n^*. We found that laminations could cause n^* values to be low in a predictable way, but also found that apparently homogeneous samples could have low n^* values. These samples with low n^* values tend to have low porosities and a high percentage of their pore volumes consisting of hairline pores along grain boundaries. We believe that these small pores remain brine saturated and well connected at the capillary pressures normally encountered in a reservoir. This leads to low n^* values. We have a fair correlation between n^* and Ø to set bounds on the range of possible values of n^*. However, we do not yet have a general formula for accurately predicting n^* in clean sandstones.

As shown herein, by Swanson (1985), and by Worthington and Pallatt (1990), heterogeneous sandstone plugs with spatially variable capillary pressures and brine saturations, cannot be expected to exhibit simple power law behavior, i.e., the RI^* versus S_w crossplots may not appear linear on log-log plots. For a curvilinear RI^* versus S_w response, it may be necessary to use another functional form or a lookup table to determine S_w from well log estimates of RI^*.

ACKNOWLEDGEMENTS

All of the data in this report were obtained using the laboratory equipment and procedures developed by Pat Worthington. Most of the measurements were made under his direction. Pat, who retired in 1988, left us with a wealth of well documented, high quality data to analyze as well as a smoothly functioning laboratory. We appreciate his contributions and dedicate this paper to him.

We thank Jim Spencer of Chevron for his careful review of this paper and his useful insights into the significance of the effects of pressure solution on the saturation exponents of low porosity sandstones. We also thank the management of Chevron for their support and permission to publish this paper.

REFERENCES

Archie, G. E., The Electrical Resistivity Log as an Aid in Determining Some Reservoir Characteristics, Trans. AIME, 146, pp54-62, 1942.

Baldwin, B. A. and Yamanashi, W. S., Persistence of Non-Uniform Brine Saturation Distribution in SCA Electrical Resistivity Core Plugs After Desaturation by Centrifuging, The Log Analyst, Vol. 30, No. 2, pp45-48, 1989.

Juhasz, I., Normalised Q_v - The Key to Shaly Sand Evaluation Using the Waxman-Smits Equation in the Absence of Core Data, Transactions SPWLA Twenty-Second Annual Logging Symposium, Paper Z, 1981.

Roberts, J. N., and Schwartz, L. M., Grain Consolidation and Electrical Conductivity in Porous Media, Phys. Rev., B31, pp5990-5997, 1985.

Schwartz, L. N., and Kimminau, S., Analysis of Electrical Conduction in the Grain Consolidation Model, Geophysics, Vol. 52, No. 10, pp1402-1411, 1987.

Shen, L. C., Liu, C., Korringa, J., and Dunn, K. J., Computation of Conductivity and Dielectric Constant of Periodic Porous Media, J. Appl. Phys. Vol. 67, No. 11, pp7071-7081, 1990.

Swanson, B. F., Microporosity in Reservoir Rocks - Its Measurement and Influence on Electrical Resistivity, Transactions SPWLA Twenty-Sixth Logging Symposium, Paper F, 1985.

Waxman, M. H., and Smits, L. J. M., Electrical Conductivities in Oil-Bearing Shaly Sands, SPE Journal, Vol. 8, pp107-122, 1968.

Worthington, P. F., and Pallatt, N., Effect of Variable Saturation Exponent Upon the Evaluation of Hydrocarbon Saturation, Transactions of SPE Sixty-Fifth Technical Conference, pp101-108, 1990.

Wyllie, M. R. J., and Gregory, A. R., Formation Factors of Unconsolidated Porous Media: Influence of Particle Shape and Effect of Cementation, Trans. AIME, 198, pp103-111, 1953.

APPENDIX: POTENTIAL MEASUREMENT ERRORS

There are potential sources of error in our saturation exponent measurements which are not fully resolved.

First, all of the measurements of $\mathbf{RI^*}$ versus S_w were done using horizontal and angle head centrifuges to lower the brine saturation in the samples. Our concern with using the centrifuge for desaturation is that non-uniform brine distributions can be established. The end of the plug further from the center of rotation will have a higher brine saturation than the end closer to the center. The use of an angle head centrifuge, where the samples are at a 45° angle to the rotation axis, further complicates the brine distribution. After the samples are removed from the centrifuge, this non-uniform saturation can persist for much longer times than originally thought (Baldwin and Yamanashi, 1989). The effect of non-uniform saturations along the length of the samples is to cause the samples to appear more resistive than they would have if the same amount of brine were uniformly distributed. We saw such an effect in chalk samples during the early 80's but were unable to determine its cause at the time. The chalks we studied possessed low permeabilities and high porosities. At the lowest centrifuge speed, a non-uniform saturation was apparently established that persisted throughout successive desaturations. The crossplots of $\mathbf{RI^*}$ versus S_w were peculiar in that the first desaturation point at S_w = 80-90% had a higher than expected value of $\mathbf{RI^*}$, but the successive points followed the usual power law behavior, i.e., fell on a straight line in the log-log crossplot. We did not see a significant tendency for this type of

behavior in our sandstone data. Still, we cannot be completely confident that our n^* values are not slightly overestimated, especially for low permeability samples.

Second, all our samples were solvent-cleaned using successively toluene, methanol and an 80/20% azeotrope of chloroform and acetone. Though not regularly tested for wettability, these samples were presumed to be strongly water-wet. Our concern is that in the reservoir, the samples may have been significantly less water-wet (i.e. larger contact angle) which would alter the brine distribution and would increase, to some unknown degree, the saturation exponent, n^*.

Third, we are concerned that the tendency of our low porosity samples to have low saturation exponents could be due to a measurement artifact. At low brine saturations, the amount of brine in samples with 10% porosity is only about 0.3 milliliters. Brine saturation is determined from weights and knowledge of the density of the brine. Any evaporation of water, will be seen as a reduction in brine saturation, but will leave the remaining brine more saline so that the resistivity will not increase as it would if both salt and water were removed. The result is a lower value of RI^* at that saturation and a consequent lowering of the value of n^*. Although evaporation is clearly a source of error during air/brine desaturation, we expect possible errors of only 0.1 or 0.2 in the value of n^*. This is based on our analysis of the following worst case example. From weights, we estimated that a sample had been desaturated to the extremely low value of $S_w = 0.01$, where some loss due to evaporation would be expected. The amount of salt remaining in the sample, as determined using an Inductively Coupled Plasma (ICP) spectrometer, was twice what we calculated assuming no evaporation. This meant that the brine saturation was slightly off and resistivity was low by a factor of two. Correcting the resistivities and brine saturations, however, changed the calculated value of n^* by less than 0.2. Thus, while the possibility of evaporation raises a question about the accuracy of RI^* measurements on low porosity samples, evaporation effects do not appear large enough to account for the strong tendency for low porosity samples to have low n^* values.

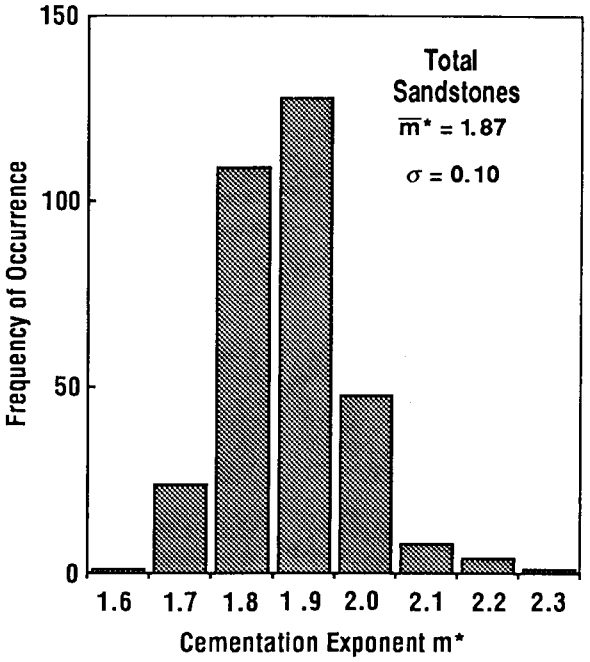

Figure 1 Data for total (11) Reservoirs.

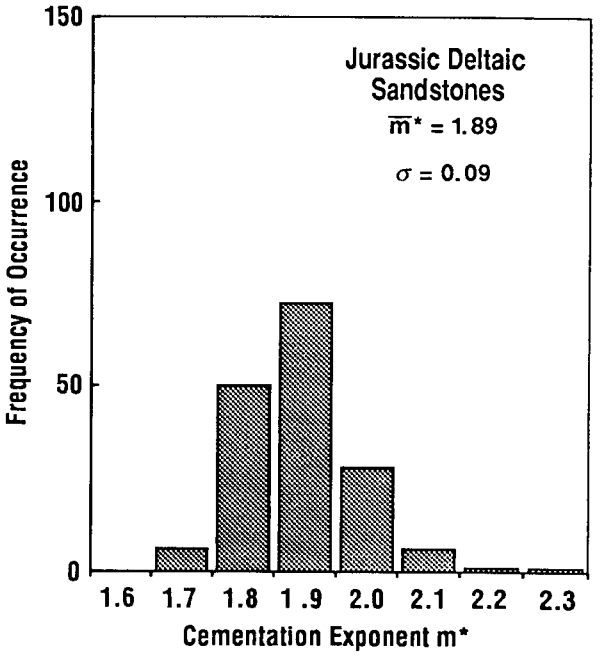

Figure 2 Reservoir A data.

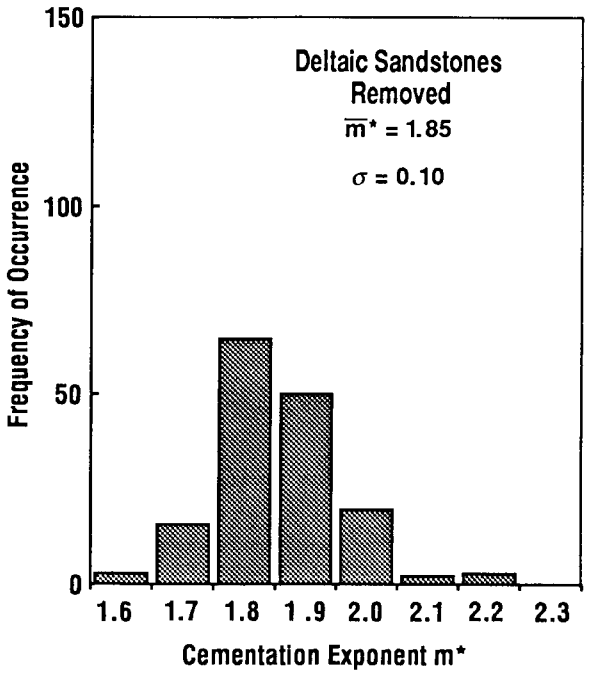

Figure 3 Total data with Reservoir A data removed.

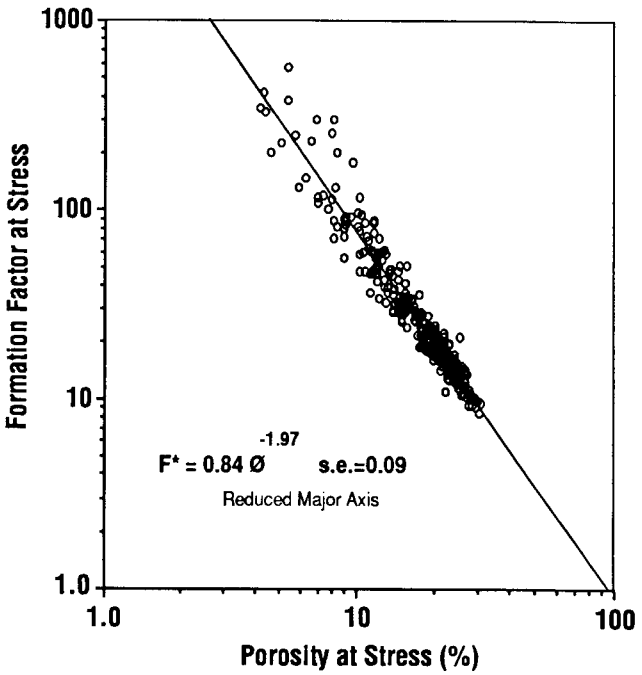

Figure 4 Formation factor versus porosity for Chevron samples.

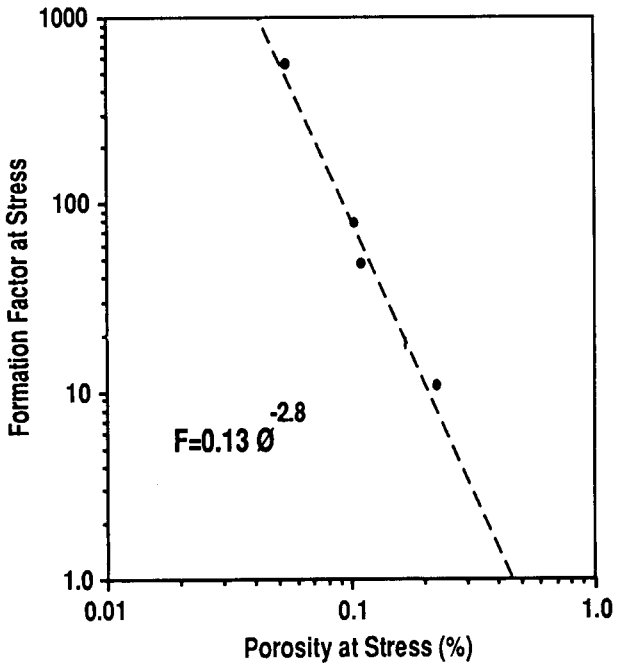

Figure 5 Crossplot of Formation Factor versus porosity for Fontainebleau sandstone.

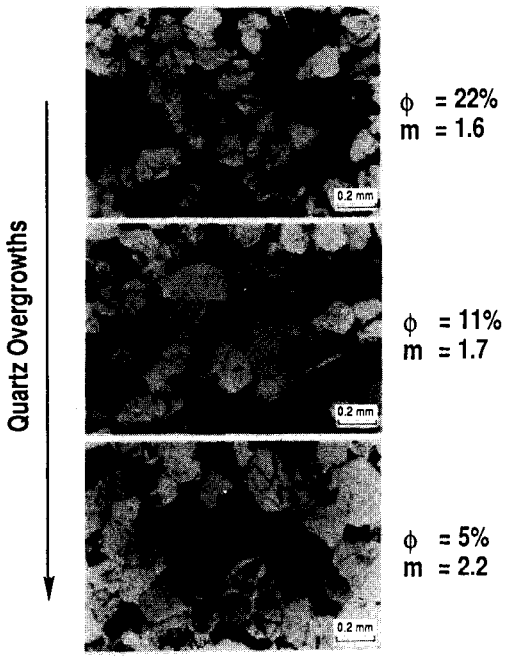

Figure 6 Quartz overgrowths lead to higher m* values.

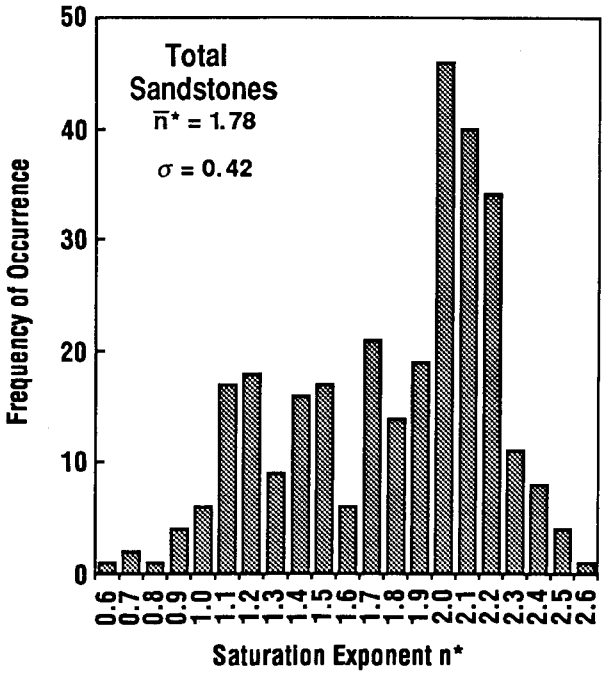

Figure 7 Data for total (11) Reservoirs.

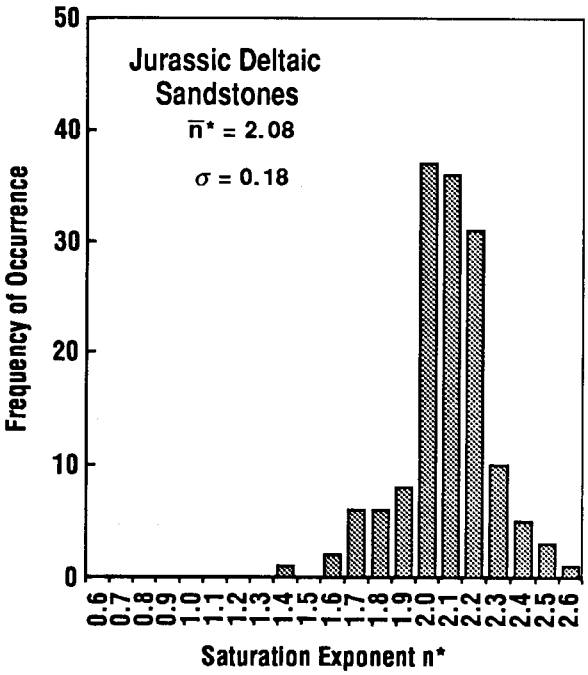

Figure 8 Reservoir A data.

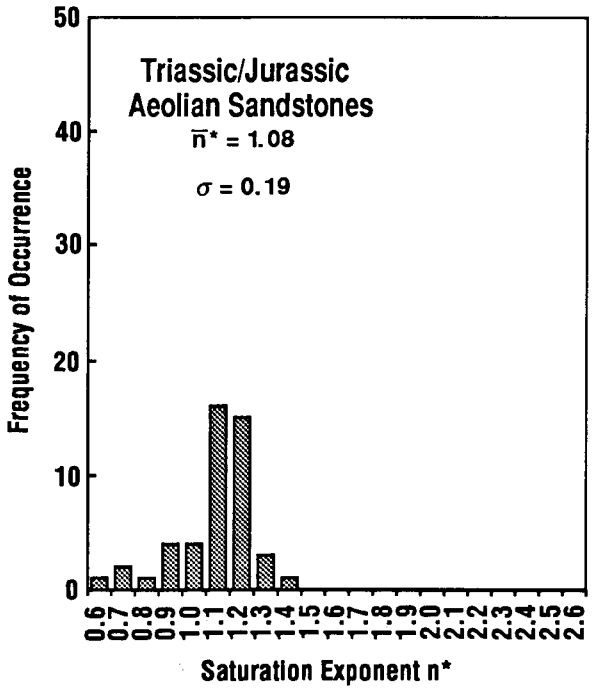

Figure 9 Reservoir B data.

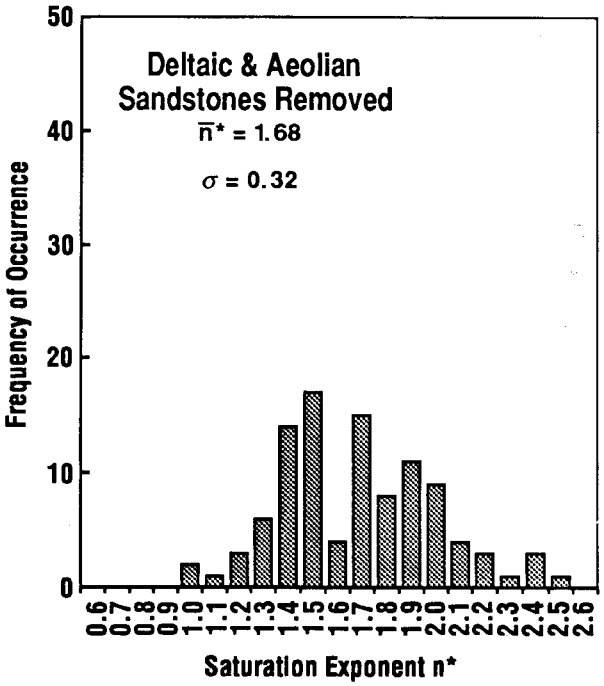

Figure 10 Reservoirs A & B data removed.

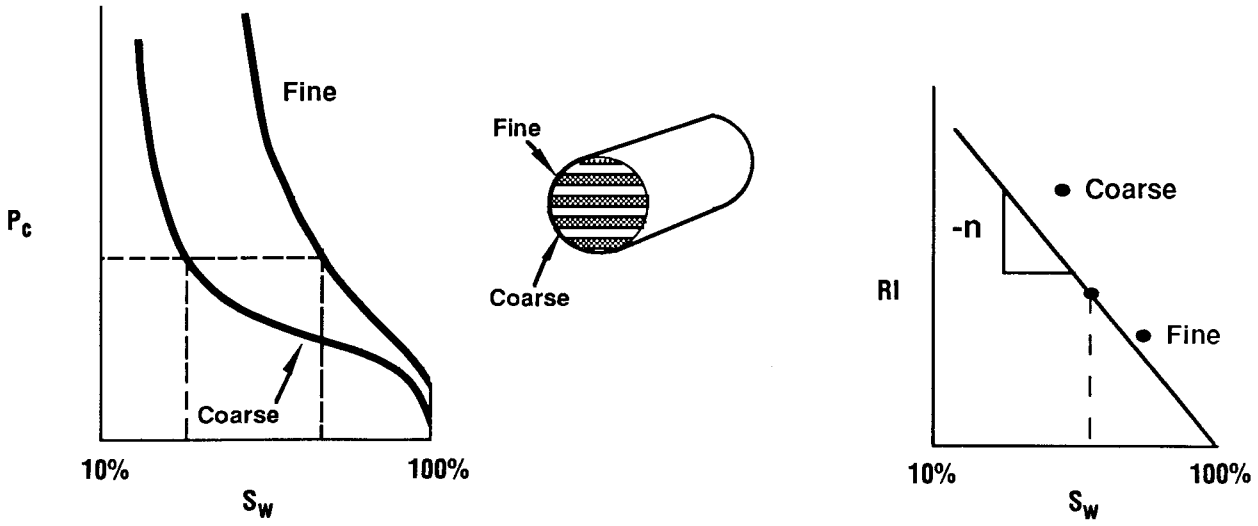

Figure 13 Laminations can lead to low values of saturation exponent n*.

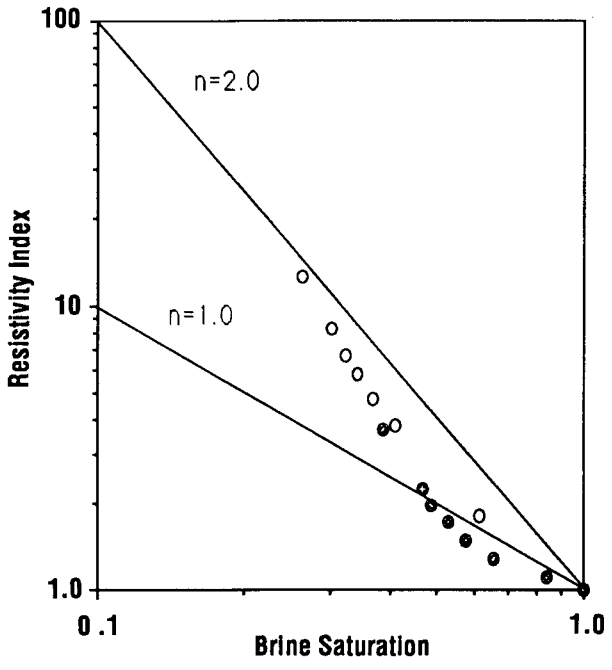

Figure 14 Resistivity Index versus brine saturation data for two laminated sandstones exhibit curvature.

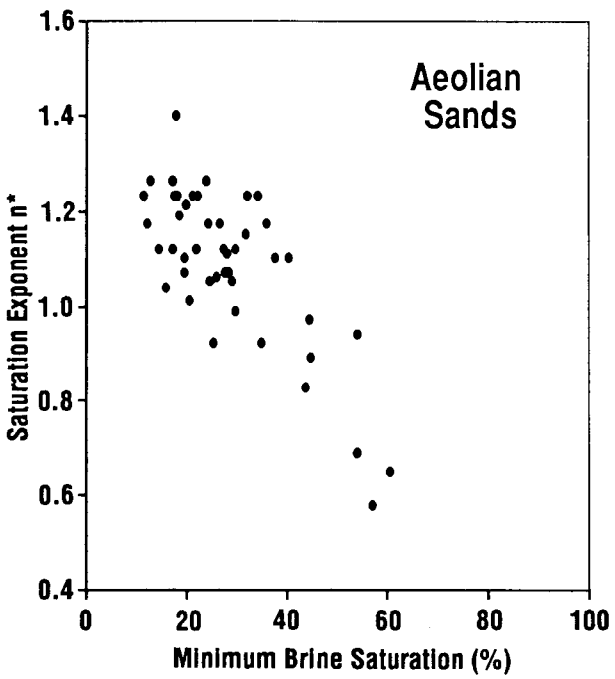

Figure 15 In aeolian sands, low values of n* tend to be associated with high values of minimum brine saturation.

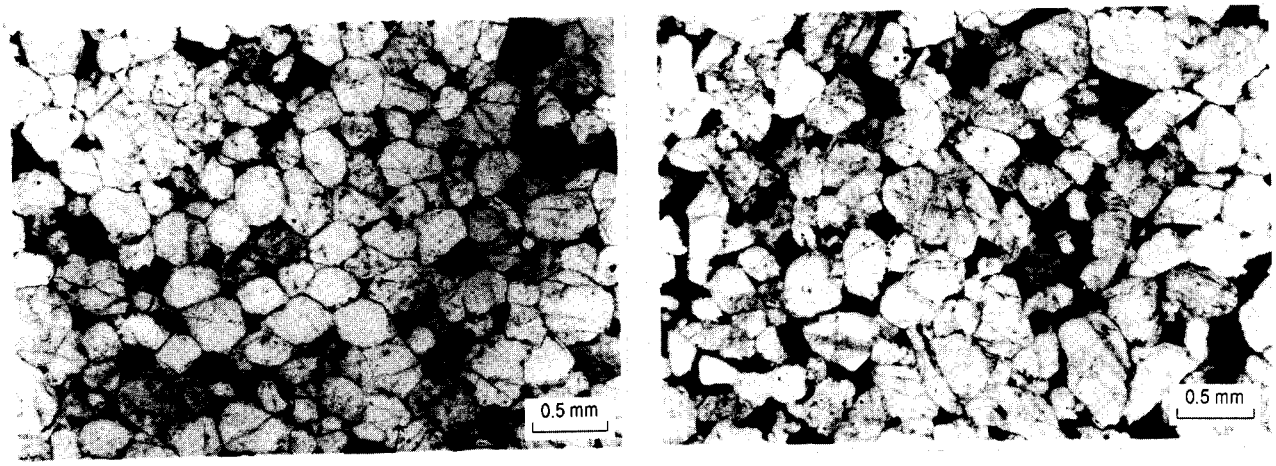

n* = 1.13
ø = 8%

n* = 0.98
ø = 11%

Figure 11 Fine-grained homogeneous sandstones with low n* values.

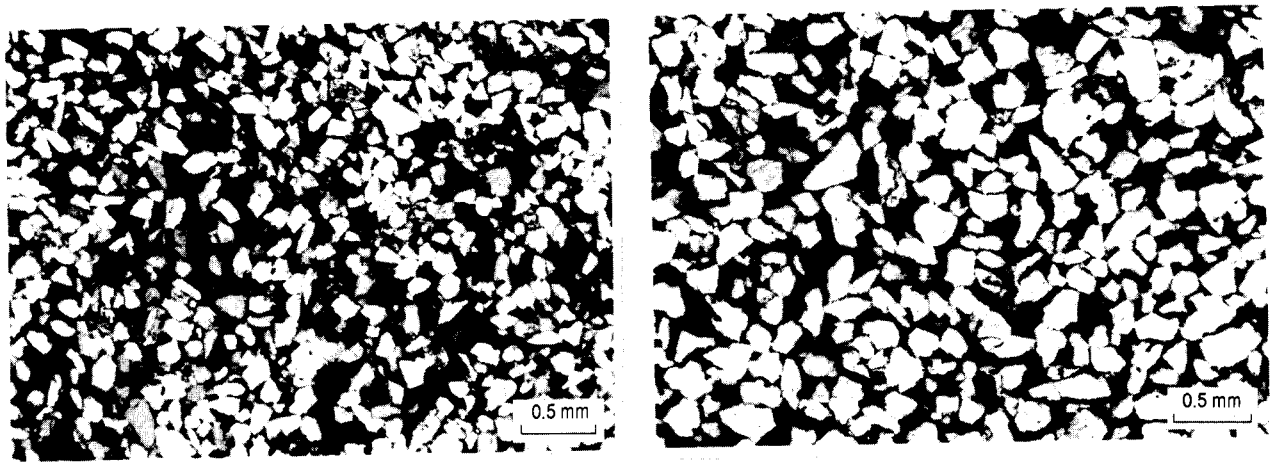

n* = 2.14
ø = 30%

n* = 2.64
ø = 25%

Figure 12 Fine-grained homogeneous sandstones with high n* values.

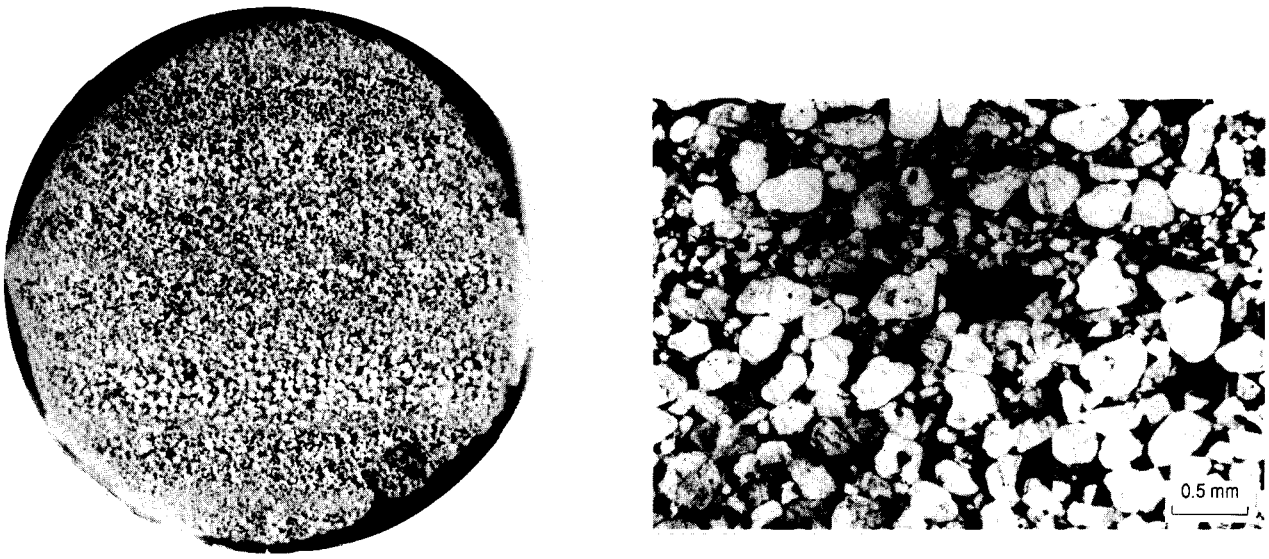

$n^* = 1.40$
$K_a = 18$ md

Figure 16 Fine to medium-grained aeolian sandstone with well-sorted laminae.

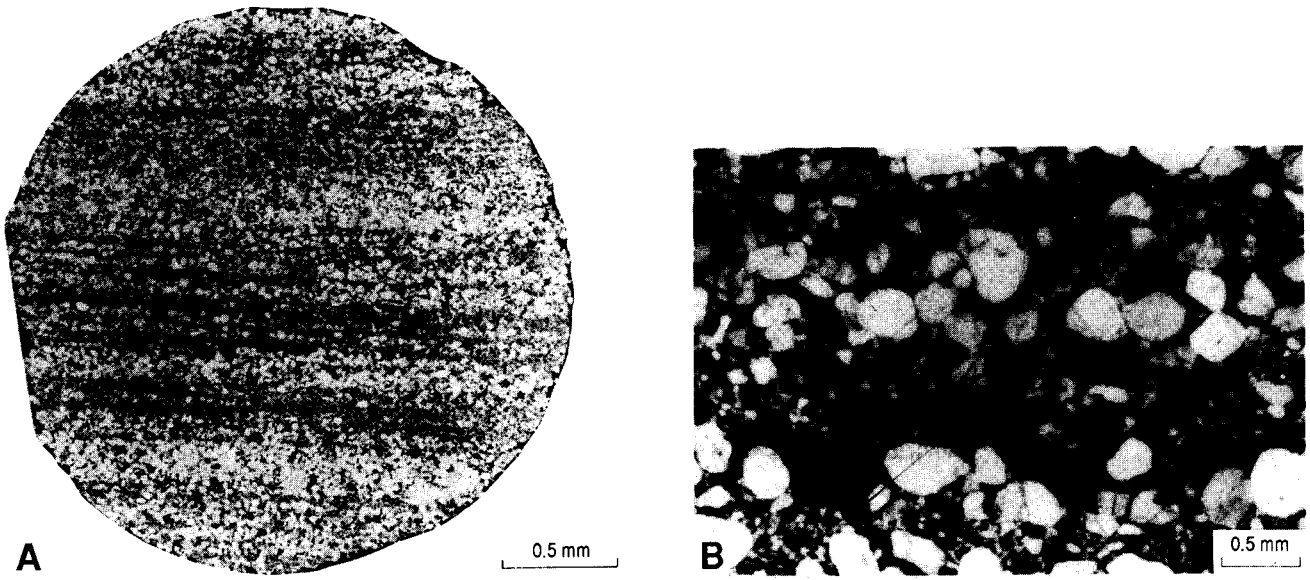

$n^* = 0.65$
$K_a = 0.09$ md

Figure 17 Very fine to medium-grained aeolian sandstone with poorly-sorted laminae.

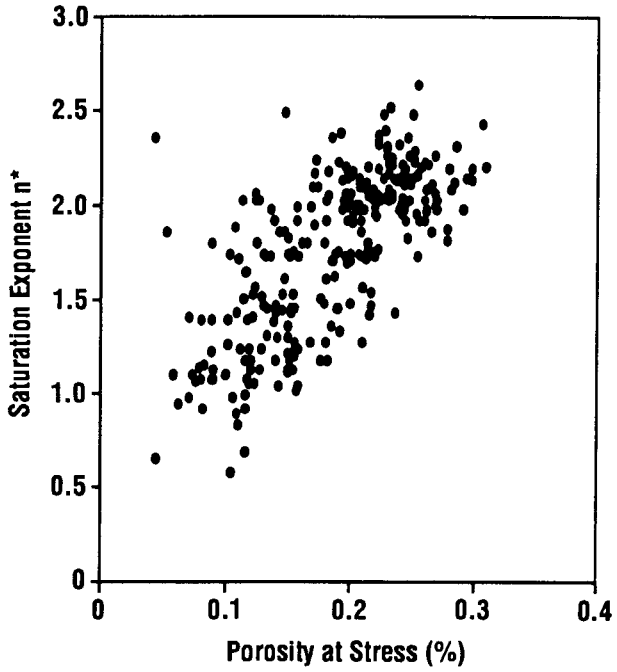

Figure 18 For the Chevron data, there is a fair correlation between porosity and n*.